# Adaptive Finite-Time Prescribed Performance Control With Small Overshoot for Uncertain 2-D Plane Vehicular Platoons

Zhenyu Gao, Zhongyang Wei, Wei Liu, and Ge Guo, *Senior Member, IEEE*

***Abstract*—This article investigates the problem of finite-time prescribed performance control for 2-D plane vehicular platoon systems with uncertain dynamics and external disturbance. First, a novel class of finite-time performance functions (FnTPFs) are designed to guarantee both spacing tracking error and bearing tracking error converge to the prescribed region within the pre-defined time with small overshoot. Then, new third-order finite-time sliding mode surfaces are designed, based on which, an improved sliding mode control scheme is established, and proved to be capable of steering the platoon tracking errors approach to small region near zero within user-defined time, while avoiding the chattering and singularity problems. Lastly, the effectiveness of the proposed scheme, together with the superiority to the existing ones, is verified by numerical simulations.**

***Index Terms*—2-D plane, vehicular platoons, sliding mode control, prescribed performance control (PPC), finite-time (FnT) control.**

## I. Introduction

In RECENT years, as one of the core technologies of the automated highway/vehicle systems, vehicular platoon control system (VPCS) has received considerable attention owing to its significant advantages in reducing exhaust emissions, increasing traffic capacity and improving road safety, and many outstanding results can be seen [1], [2], [3], [4], [5] and their references. For a platoon task, each vehicle is required to track the vehicle in front of it with an appropriate spacing strategy under a specific communication topology [6], [7]. At present, there are two major spacing strategies, namely, constant spacing (CS) [8] and constant time-headway spacing (CTH) [9], along with the two most commonly used communication topology, including the leader-predecessor following [10] and predecessor-following [11].

Received 8 May 2024; revised 9 September 2024; accepted 12 September 2024. Date of publication 18 September 2024; date of current version 16 January 2025. This work was supported in part by the National Natural Science Foundation of China under Grant 62303101 and in part by the Natural Science Foundation of Hebei Province under Grant F2023501001. The review of this article was coordinated by Prof. Shahid Mumtaz. *(Corresponding author: Ge Guo.)*

Zhenyu Gao, Zhongyang Wei, and Wei Liu are with the School of Control Engineering, Northeastern University at Qinhuangdao, Qinhuangdao 066004, China (e-mail: 18840839109@163.com; 15953603659@163.com; liu_w1999@163.com).

Ge Guo is with the State Key Laboratory of Synthetical Automation for Process Industries, Northeastern University, Shenyang 110819, China (e-mail: geguo@yeah.net).

Digital Object Identifier 10.1109/TVT.2024.3463635

Avoiding collision and maintaining communication connectivity among adjacent vehicles are practice and common problems in VPCS, which play an crucial role in vehicular platoon safety [12], [13]. In other words, only if the above two problems, that is, collision avoidance and connectivity preservation, are dealt with, the platoon goal can be successfully achieved, otherwise it will fail. For this purpose, many effective methods, such as the barrier Lyapunov function method (BLF) [14], [15], the prescribed performance control (PPC) [16] method, and so on, have been developed. Among them, the PPC method, thanks to its simple design and low computational effort, has become the most widely used algorithm [17], [18], [19]. Lately, based on finite-time performance functions (FnTPFs) [20], [21] or fixed-time performance functions (FxTPFs) [22], [23], many advance PPC methods are designed to ensure the tracking errors converge to a predefined steady state region within a given time.

The above results were only applied to the 1-D plane vehicular platoons, yet many application scenarios in reality are in the 2-D plane [24], [25], [26], such as tunnels, ramps, passing through construction sections, etc., which are seldom taken into account. In [27], based on conventional performance function, a PPC method is proposed for vehicular platoons with performance constraints on the 2-D plane for the first time. Further, the authors of [27] developed a novel PPC method, on the basis of FnTPFs, for 2-D plane vehicle platoons [28]. Although, the PPC method proposed in [28] guarantees that the tracking error can approach to a prescribed region for a user-designed time, but the boundaries of the performance function are on both sides of the origin and are fixed, which increases the overshoot of the VPCS. To the best of author's knowledge, the PPC method that enables tracking errors to have small overshoot and converge to a predefined region for a pre-defined time simultaneously has not been carried out for 2-D plane vehicular platoons.

Motivated by the above discussions, this article proposes a new finite-time prescribed performance control framework for 2-D plane nonlinear vehicular platoons. To be specific, two pairs of FnTPFs are introduced to prescribe both transient and steadstate performances by establishing tracking error constraints. Then, based on error transformation mechanism, a new sliding mode control method is designed for 2-D plane third-order nonlinear vehicular platoons. In comparison with the latest

TABLE I
DEFINITIONS OF THE MODEL PARAMETERS

| Parameter | Description | Unit |
|---|---|---|
| $m_i$ | Vehicle's mass | $kg$ |
| $g$ | Acceleration of gravity | $m/s^2$ |
| $\delta_i$ | Road slope angle | $rad$ |
| $\rho_{ai}$ | Air density | $kg/m^3$ |
| $A_i$ | Frontal cross-area | $m^2$ |
| $\tau_i$ | Engine time constant | $s$ |
| $C_{ai}$ | Drag coefficient | - |
| $b_i$ | Road resistance coefficient | - |
| $d_{d_i}$ | the disturbance on throttle/brake | - |
| $d_{\phi_i}$ | the disturbance on steering wheel | - |

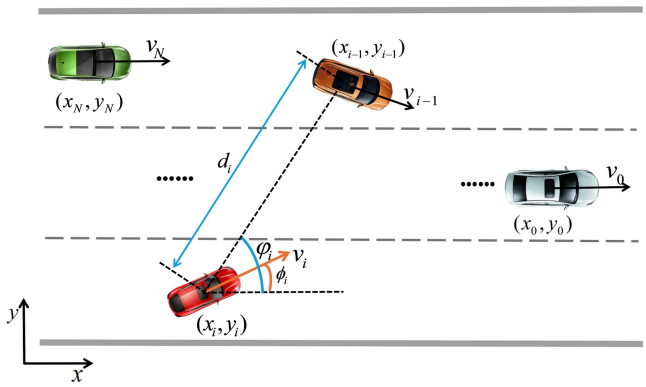


Fig. 1. The 2-D plane vehicular platoon configuration.

results, the superiorities of this article can be summarized as follows:

1) Two pairs of finite-time prescribed performance functions (FnTPFs) are defined, based on which a novel finite-time PPC scheme is constructed to ensure collision avoidance and connectivity preservation between neighboring vehicles. Compared with the existing results [17], [18], [19], [20], [21], [22], [23], [27], [28], [31], the developed PPC method can guarantee that the tracking errors converge to a preset region for a user-designed time and has small overshoot.
2) Since the works [27], [28], [32], [33], [34], [35] also research the finite-time platoon control of vehicles, but the given second-order sliding mode surfaces cannot be directly applied to the third-order vehicle platoons. Thus, this paper first proposes a finite-time control scheme based on a novel third-order finite-time sliding-mode surface for the 2-D vehicular platoons. The suggested scheme ensures that the tracking error converge to a given region within a finite time, which only determined by the control parameters, while eliminating the singularity problem, reducing the system chattering, and improving the convergence rate of the system.

*Notation:* Throughout this paper, $|\cdot|$ denotes the absolute value of a real number, $\text{sig}^*(\bullet) = |\bullet|^*\text{sign}(\bullet)$, $\mathcal{V}_N = \{1, 2, \ldots, N\}$ represents the integer set from 1 to $N$. Moreover, the continuous-time argument $(t)$ is omitted for the simplicity in some case.

## II. Problem Formulation and Preliminaries

### A. Vehicle Dynamics

Different from [20], [21], [29], [30], this paper considers a 2-D plane vehicular platoon consisting one leader (labeled 0) and $N$ following vehicles (see Fig. 1). The following third-order dynamics model is introduced for the vehicle $i$ ($i \in \mathcal{V}_N$):

$$\begin{cases} \dot{x}_i(t) = v_i(t)\cos(\phi_i(t)), \\ \dot{y}_i(t) = v_i(t)\sin(\phi_i(t)), \\ \dot{v}_i(t) = a_i(t), \\ \dot{a}_i(t) = \frac{1}{m_i\tau_i}u_{d_i}(t) + f_i(x_i, y_i, v_i, a_i) + d_{d_i}(t) \\ \dot{\phi}_i(t) = \omega_i(t) \\ \dot{\omega}_i(t) = \varpi_i(t) \\ \dot{\varpi}_i(t) = u_{\phi_i}(t) + d_{\phi_i}(t) \end{cases} \tag{1}$$

with

$$f_i(x_i, y_i, v_i, a_i) = -\frac{1}{m_i\tau_i}\left[\rho_{ai}A_iC_{a_i}\left(\frac{1}{2}v_i^2 + \tau_i v_i a_i\right) + m_i g b_i\cos\delta_i + m_i g\sin\delta_i\right] - \frac{1}{\tau_i}a_i$$

where $x_i$, $y_i$, $\phi_i$, $v_i$, $\omega_i$, $a_i$ and $\varpi_i$ denote the vehicle's longitudinal position, transverse position, heading angle, velocity, angle rate, acceleration, and angular acceleration, respectively, $u_{d_i}$ is the throttle/brake input, $u_{\phi_i}$ being the steering wheel input, $f_i(x_i, y_i, v_i, a_i)$ is the unknown unmodeled dynamics, and the definition of other parameters are given in Table I.

Inspired by [36], rewrite $f_i(x_i, y_i, v_i, a_i)$ as:

$$f_i(x_i, y_i, v_i, a_i) = f_{i0}(x_i, y_i, v_i, a_i) + \Delta f_i(x_i, y_i, v_i, a_i) \tag{2}$$

where $f_{i0}(x_i, y_i, v_i, a_i)$ and $\Delta f_i(x_i, y_i, v_i, a_i)$ represent the known term and the uncertain term, respectively.

Based on (2), the third equation in (1) becomes:

$$\dot{a}_i(t) = \frac{1}{m_i\tau_i}u_{d_i}(t) + f_{i0}(x_i, y_i, v_i, a_i) + D_i(t) \tag{3}$$

where $D_i = \Delta f_i(x_i, y_i, v_i, a_i) + d_{d_i}(t)$ stands for the lumped disturbance acting on vehicle $i$.

*Assumption 1:* $D_i$ and $d_{\phi_i}$ are bounded and satisfy $|D_i| \le D_{i0}$, $|d_{\phi_i}| \le d_{\phi_{i0}}$ with $D_{i0}$ and $d_{\phi_{i0}}$ are unknown positive constants.

For the leader, the dynamics model is adopted as follows:

$$\begin{cases} \dot{x}_0(t) = v_0(t)\cos(\phi_0(t)) \\ \dot{y}_0(t) = v_0(t)\sin(\phi_0(t)) \\ \dot{v}_0(t) = a_0(t) \\ \dot{\phi}_0(t) = \omega_0(t) \\ \dot{\omega}_0(t) = \varpi_0(t) \end{cases} \tag{4}$$

*Remark 1:* In order to accomplish tasks in a 2-dimensional scenario, such as multi-lane vehicle merging (see Fig. 2), lane changing (see Fig. 3), etc., this paper adopts the dynamics

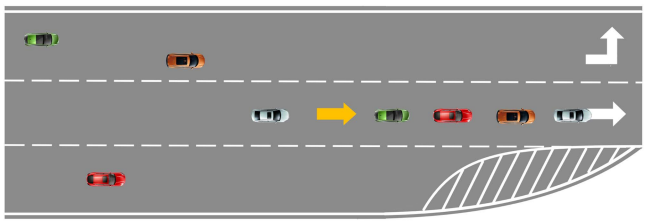

Fig. 2. Multilane vehicle merging.

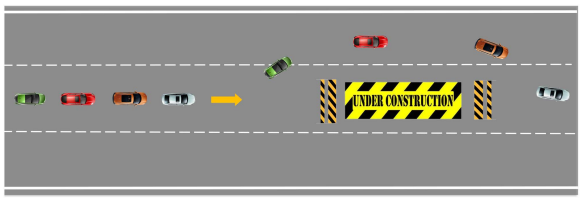


Fig. 3. Vehicular platoon lane changing.

models (1) and (4), which is more complex and realistic than the conventional 1-D platoon dynamics model in [3], [4], [5], [6], [7], [8], [9], [10], [11], [12], [13], [14], [15], [16], [17], [18], [19], [20], [21], [22], [23]. In addition, unlike the second-order nonlinear models in [27], [38], a more accurate third-order 2-D plane nonlinear vehicle model considering the engine dynamics is proposed in this paper.

### B. Platoon Control in 2-D Plane

As shown in Fig. 1, the spacing distance $d_i(t)$ and the bearing angle $\varphi_i(t)$ between vehicle $i$ and vehicle $i-1$ with $i \in \mathcal{V}_N$ are defined as follows:

$$d_i(t) = \sqrt{(x_{i-1} - x_i)^2 + (y_{i-1} - y_i)^2} \tag{5}$$

$$\varphi_i(t) = \arctan\left(\frac{y_{i-1} - y_i}{x_{i-1} - x_i}\right) \tag{6}$$

otherwise, $\varphi_i(t) = \frac{\pi}{2}$.

As described before, collision avoidance and communication connection among adjacent vehicles should be guaranteed, thus the spacing distance $d_i$ must meet the following constraints:

$$0 < d_{i\min} < d_i < d_{i\max}, i \in \mathcal{V}_N \tag{7}$$

where $d_{i\min}$ and $d_{i\max}$ denote the minimum safe distance and the maximum effective communication distance, respectively.

Based on (5) and (7), the spacing tracking error $e_{d_i}$ and the bearing angle tracking error $e_{\phi_i}(t)$ are defined as:

$$e_{d_i} = d_i - d_i^* \tag{8}$$

$$e_{\phi_i} = \phi_i - \varphi_i \tag{9}$$

where $d^*$ is the desired spacing, and satisfies $0 < d_{i\min} < d_i^* < d_{i\max}$. Furthermore, the variation range for the velocity angle is set as: $\phi_i \in [-\pi, \pi]$.

According to (8), we further have:

$$-\underline{\Lambda}_i < e_{d_i} < \overline{\Lambda}_i \tag{10}$$

with $\underline{\Lambda}_i = d_i^* - d_{i\min}$ and $\overline{\Lambda}_i = d_{i\max} - d_i^*$.

### C. Control Objectives

In this paper, we aim to design a novel control scheme for each following vehicle described by (1) and (4) such that the two objectives given below can be met.

1) All internal signals in the vehicular platoon system are bounded in finite-time.
2) The spacing tracking error $e_{d_i}(t)$ converge to a given region within a user-defined time, which implies

$$-\epsilon_i < e_{d_i}(t) < \epsilon_i, \forall t \geq \tilde{T}_i \tag{11}$$

where $\epsilon_i$ and $\tilde{T}_i$ are positive constants, and can be predefined.
3) Weak string stability of the vehicular platoon system is also guaranteed in finite time.

### D. Preliminaries

*Lemma 1:* [37] Consider the system $\dot{x} = f(x)$ with $x(0) = x_0$ and the positive-definite function $V(x)$. If $\dot{V}(x) \leq -k_1 V(x) - k_2 V^{\gamma}(x) + \omega$ with $k_1 > 0$, $k_2 > 0$, $0 < \gamma < 1$ and $0 < \omega < \infty$, then $\dot{x} = f(x)$ is practically finite-time stable (PFnTS), and the convergence region of system $\dot{x} = f(x)$ is given by

$$\lim_{t \to T} |V(x) \leq \min\left\{\frac{\omega}{\left(1-\tilde{\theta}\right)k_1}, \left(\frac{\omega}{\left(1-\tilde{\theta}\right)k_2}\right)^{\frac{1}{\gamma}}\right\} \tag{12}$$

with $\tilde{\theta}$ satisfies $0 < \tilde{\theta} < 1$. The convergence time is bounded by

$$T \leq \max\left\{\frac{1}{\tilde{\theta}k_1(1-\gamma)} \ln \frac{\tilde{\theta}k_1 V^{1-\gamma}(0) + k_2}{k_2}, \right.$$
$$\left. \frac{1}{k_1(1-\gamma)} \ln \frac{k_1 V^{1-\gamma}(0) + \tilde{\theta}k_2}{\tilde{\theta}k_2}\right\}. \tag{13}$$

*Lemma 2:* [20] Let $\xi_1, \xi_2, \ldots, \xi_N \leq 0$, then

$$\sum_{i=1}^{N} \xi_i^p \geq \left(\sum_{i=1}^{N} \xi_i\right)^p, 0 < p \leq 1 \tag{14}$$

*Lemma 3:* [20] For $s \leq c$, $c > 0$, $q > 0$, $k > 0$, $p \geq 0$, we have:

$$s^{1+k} - c^{1+k} \leq (c-s)^{1+k},$$
$$p^k (q-p) \leq \frac{1}{1+k}\left(q^{1+k} - p^{1+k}\right). \tag{15}$$

*Lemma 4:* [20] Let $a \in R$, $b \in R$, and $c > 1$, $d > 1$ be two real numbers with $(c-1)(d-1) = 1$. For any $\varepsilon > 0$, one has

$$ab \leq \frac{\varepsilon^c}{c}|a|^c + \frac{1}{d\varepsilon^d}|b|^d. \tag{16}$$

*Definition 1:* (Weak String Stability [8]): The platooning system is weak string stable in terms of the spacing error $e_{d_i}$, if given any $\epsilon > 0$, there exists $\Delta > 0$ such that $\|e_{d_i}(0)\| < \Delta \Rightarrow \sup_i \|e_{d_i}(\cdot)\|_\infty < \epsilon$.

## III. Main Results

In this section, the main results, including prescribed performance transformation, finite-time sliding mode controller design and stability analysis, are proposed.

### A. Prescribed Performance Control

*1) Finite-Time Performance Function Design:* To meet the error constrain (11), the PPC requirement can be expressed as the following time-varying constrains:

$$\begin{cases} \overline{B}_i(t) < e_{d_i}(t) < \overline{A}_i(t), & e_{d_i}(0) \geq 0 \\ \underline{A}_i(t) < e_{d_i}(t) < \underline{B}_i(t), & e_{d_i}(0) < 0 \end{cases} \tag{17}$$

were $\overline{A}_i(t)$, $\overline{B}_i$, $\underline{B}_i$ and $\underline{A}_i(t)$ denote the performance functions. Based on (10) and (11), two new kinds of finite-time performance function are designed:

$$\overline{A}_i(t) = \begin{cases} (\overline{\Lambda}_i - \epsilon_i)\dfrac{1-\frac{t}{\tilde{T}_i}}{\ln\left(e+\frac{\tilde{T}_i t}{\tilde{T}_i - t}\right)} + \epsilon_i, & 0 \leq t \leq \tilde{T}_i \\ \epsilon_i, & t > \tilde{T}_i \end{cases} \tag{18}$$

$$\underline{A}_i(t) = \begin{cases} (-\underline{\Lambda}_i + \epsilon_i)\dfrac{1-\frac{t}{\tilde{T}_i}}{\ln\left(e+\frac{\tilde{T}_i t}{\tilde{T}_i - t}\right)} - \epsilon_i, & 0 \leq t \leq \tilde{T}_i \\ -\epsilon_i, & t > \tilde{T}_i \end{cases} \tag{19}$$

$$\overline{B}_i(t) = \begin{cases} (e_{d_i}(0) - \delta_i + \epsilon_i)\frac{\tilde{T}_i - t}{\tilde{T}_i}\exp\left(\frac{-t}{\tilde{T}_i - t}\right) - \epsilon_i, & 0 \leq t \leq \tilde{T}_i \\ -\epsilon_i, & t > \tilde{T}_i \end{cases} \tag{20}$$

$$\underline{B}_i(t) = \begin{cases} (e_{d_i}(0) + \delta_i - \epsilon_i)\frac{\tilde{T}_i - t}{\tilde{T}_i}\exp\left(\frac{-t}{\tilde{T}_i - t}\right) + \epsilon_i, & 0 \leq t \leq \tilde{T}_i \\ \epsilon_i, & t > \tilde{T}_i \end{cases} \tag{21}$$

where $\tilde{T}_i$, $\delta_i$ and $\epsilon_i$ are the designed positive parameters with $0 < \epsilon_i < \min\{\underline{\Lambda}_i, \overline{\Lambda}_i\}$, and $|e_{d_i}(0)| \geq \delta_i$.

*Remark 2:* Based on (17)–(21), it is obviously that $0 \leq \bar{B}_i(0) < \bar{A}_i(0)$ and $\underline{A}_i(0) < \underline{B}_i(0) \leq 0$, which means that the boundaries of the selected performance functions are on the same side at the initial time. Compared to [28], the PPC method proposed in this paper limits the tracking error to a relatively narrow area, resulting in smaller system overshoot and faster convergence rate.

*2) Error Transformation:* As mentioned in [21], designing the controller based directly on constrained tracking error (17) is rendered extremely difficult, thus the following error transformation is introduced, based on which the constrained error can be transformed into unconstrained one:

$$e_{d_i}(t) = \begin{cases} K\left(\mathcal{E}_i(t)\right)\left(\overline{A}_i(t) - \overline{B}_i(t)\right) + \overline{B}_i(t), e_{d_i}(0) \geq 0 \\ K\left(\mathcal{E}_i(t)\right)\left(\underline{A}_i(t) - \underline{B}_i(t)\right) + \underline{B}_i(t), e_{d_i}(0) < 0 \end{cases} \tag{22}$$

where $\mathcal{E}_i(t)$ is the transformed error, $K(\mathcal{E}_i(t))$ is a smooth strictly increasing invertible function, which should meet the following conditions:

$$\begin{cases} \lim_{\mathcal{E}_i(t)\to-\infty} K\left(\mathcal{E}_i(t)\right) = 0, \\ \lim_{\mathcal{E}_i(t)\to+\infty} K\left(\mathcal{E}_i(t)\right) = 1, \end{cases} \quad e_{d_i}(0) \geq 0, \tag{23}$$

$$\begin{cases} \lim_{\mathcal{E}_i(t)\to-\infty} K\left(\mathcal{E}_i(t)\right) = 1, \\ \lim_{\mathcal{E}_i(t)\to+\infty} K\left(\mathcal{E}_i(t)\right) = 0, \end{cases} \quad e_{d_i}(0) < 0. \tag{24}$$

According to (23) and (24), the following function $K(\mathcal{E}_i(t))$ is selected:

$$K\left(\mathcal{E}_i(t)\right) = \begin{cases} \frac{e^{\mathcal{E}_i(t)}}{1+e^{\mathcal{E}_i(t)}}, & e_{d_i}(0) \geq 0 \\ \frac{1}{1+e^{\mathcal{E}_i(t)}}, & e_{d_i}(0) < 0 \end{cases} \tag{25}$$

By inverse transformation, the transformed error $\mathcal{E}_i(t)$ can be expressed as:

$$\mathcal{E}_i(t) = \begin{cases} \ln\left(\frac{e_{d_i}(t)-\overline{B}_i}{\overline{A}_i - e_{d_i}(t)}\right), & e_{d_i}(0) \geq 0 \\ \ln\left(\frac{e_{d_i}(t)-\underline{A}_i(t)}{\underline{B}_i(t) - e_{d_i}(t)}\right), & e_{d_i}(0) < 0 \end{cases} \tag{26}$$

Here, it should be noted that the two variables $e_{d_i}(t)$ and $\mathcal{E}_i(t)$ are equivalent and have the same convergence property, which means that the convergence of $e_{d_i}(t)$ can be achieved provided that $\mathcal{E}_i(t)$ is convergent.

For the following controller design, taking the first-order and second-order derivatives of $\mathcal{E}_i(t)$ with respect to time $t$, we have:

$$\begin{aligned} \dot{\mathcal{E}}_i(t) &= R_i\left(\dot{e}_{d_i}(t) + \sigma_i\right) \\ \ddot{\mathcal{E}}_i(t) &= R_i\left(\ddot{e}_{d_i}(t) + \dot{\sigma}_i\right) + \dot{R}_i\left(\dot{e}_{d_i}(t) + \sigma_i\right) \end{aligned} \tag{27}$$

with

$$\begin{aligned} \dot{e}_{d_i} = \frac{1}{d_i}\Big[&(x_{i-1} - x_i)\left[v_{i-1}\cos\left(\phi_{i-1}\right) - v_i\cos\left(\phi_i\right)\right] \\ &+ (y_{i-1} - y_i)\left[v_{i-1}\sin(\phi_{i-1}) - v_i\sin(\phi_i)\right]\Big] \end{aligned} \tag{28}$$

$$\ddot{e}_{d_i} = \frac{\Gamma_i - \dot{e}_{d_i}^2}{d_i} - a_i X_i \tag{29}$$

where $R_i$, $\sigma_i$, $\Gamma_i$ and $X_i$ are expressed as follows:

$$R_i = \begin{cases} \frac{\overline{A}_i(t)-\overline{B}_i(t)}{\left(e_{d_i}(t)-\overline{B}_i(t)\right)\left(\overline{A}_i(t)-e_{d_i}(t)\right)}, e_{d_i}(0) \geq 0 \\ \frac{\underline{B}_i(t)-\underline{A}_i(t)}{\left(e_{d_i}(t)-\underline{A}_i(t)\right)\left(\underline{B}_i(t)-e_{d_i}(t)\right)}, e_{d_i}(0) < 0 \end{cases} \tag{30}$$

$$\sigma_i = \begin{cases} \frac{\dot{\overline{B}}_i(t)-\dot{\overline{A}}_i(t)}{\overline{A}_i(t)-\overline{B}_i(t)}e_{d_i}(t) + \frac{\overline{B}_i(t)\dot{\overline{A}}_i(t)-\dot{\overline{B}}_i(t)\overline{A}_i(t)}{\overline{A}_i(t)-\overline{B}_i(t)}, e_{d_i}(0) \geq 0 \\ \frac{\dot{\underline{A}}_i(t)-\dot{\underline{B}}_i(t)}{\underline{B}_i(t)-\underline{A}_i(t)}e_{d_i}(t) + \frac{\underline{A}_i(t)\dot{\underline{B}}_i(t)-\dot{\underline{A}}_i(t)\underline{B}_i(t)}{\underline{B}_i(t)-\underline{A}_i(t)}, e_{d_i}(0) < 0 \end{cases} \tag{31}$$

$$\begin{aligned}\Gamma_i = &(x_{i-1}-x_i)\left[-v_{i-1}\omega_{i-1}\sin(\phi_{i-1})+v_i\omega_i\sin(\phi_i)\right.\\ &+\left.\dot{v}_{i-1}\cos(\phi_{i-1})\right]+(y_{i-1}-y_i)\left[v_{i-1}\omega_{i-1}\cos(\phi_{i-1})\right.\\ &-\left.v_i\omega_i\cos(\phi_i)+\dot{v}_{i-1}\sin(\phi_{i-1})\right]+\left[v_{i-1}\cos(\phi_{i-1})\right.\\ &-\left.v_i\cos(\phi_{i-1})\right]^2+\left[v_{i-1}\sin(\phi_{i-1})-v_i\sin(\phi_i)\right]^2\\ X_i = &\frac{\cos(\phi_i)(x_{i-1}-x_i)+\sin(\phi_i)(y_{i-1}-y_i)}{d_i}\end{aligned}$$

and $R_i > 0$.

### B. Finite-Time Tracking Controller Design

In this subsection, a novel finite-time sliding mode controller is proposed for every following vehicle.

*1) Finite-Time Sliding Mode Surface Design:* Inspired by [21], [39], the following finite-time sliding mode surfaces with faster convergence rate are considered:

$$S_{d_i} = \ddot{\mathcal{E}}_i(t) + c_2\text{sign}(\dot{\mathcal{E}}_i)\left|\dot{\mathcal{E}}_i\right|^{a_2} + c_1\Upsilon_i(\mathcal{E}_i) \tag{32}$$

$$S_{\phi_i} = \ddot{e}_{\phi_i} + \varrho_2\text{sign}(\dot{e}_{\phi_i})\left|\dot{e}_{\phi_i}\right|^{a_2} + \varrho_1\Upsilon_i(e_{\phi_i}) \tag{33}$$

with $\Upsilon_i(\mathcal{E}_i)$ and $\Upsilon_i(e_{\phi_i})$ are designed as:

$$\Upsilon_i(\mathcal{E}_i) = \begin{cases}\text{sig}^{a_1}(\mathcal{E}_i), |\mathcal{E}_i| \geq \iota_i\\ \alpha_1\mathcal{E}_i + \alpha_2\mathcal{E}_i^2\text{sign}(\mathcal{E}_i), |\mathcal{E}_i| < \iota_i\end{cases}$$

$$\Upsilon_i(e_{\phi_i}) = \begin{cases}\text{sig}^{a_1}(e_{\phi_i}), |e_{\phi_i}| \geq \varsigma_i\\ \beta_1 e_{\phi_i} + \beta_2 e_{\phi_i}^2\text{sign}(e_{\phi_i}), |e_{\phi_i}| < \varsigma_i\end{cases} \tag{34}$$

where $\iota_i > 0$, $\alpha_1 = (2-a_1)\iota_i^{a_1-1}$, $\alpha_2 = (a_1-1)\iota_i^{a_1-2}$, $\beta_1 = (2-a_1)\varsigma_i^{a_1-1}$, $\beta_2 = (a_1-1)\varsigma_i^{a_1-2}$. $c_1$, $c_2$, $\varrho_1$ and $\varrho_2$ are positive parameters such that the polynomials $p^2 + c_2p + c_1$ and $p^2 + \varrho_2p + \varrho_1$ are Hurwitz. In addition, $a_1$ and $a_2$ can be determined based on the following conditions [39]:

$$\begin{cases}a_1 = \dfrac{a_2}{2-a_2}\\ a_2 = a\end{cases} \tag{35}$$

with $a \in (0,1)$. The above parameters need to be designed to ensure that the sliding surface converges in finite time.

*Remark 3:* In comparison with the linear third-order sliding mode surfaces in [28], here, drawing inspiration from [21], a novel third-order sliding mode surfaces in (32) and (33) are constructed in terminal sliding mode form, based on which the tracking errors converge to origin along the sliding mode surface in finite time with faster convergence rate, while avoiding the chattering and singularity issues.

*2) Finite-Time Sliding Mode Controller Design:* To guarantee the convergence $S_{d_i}$ and $S_{\phi_i}$, taking the time derivative of $S_{d_i}$ and $S_{\phi_i}$ yields:

$$\dot{S}_{d_i} = \dddot{\mathcal{E}}_i + \dot{\chi}_i + c_1\dot{\Upsilon}_i(\mathcal{E}_i) \tag{36}$$

$$\dot{S}_{\phi_i} = \dddot{e}_{\phi_i} + \dot{N}_i + \varrho_1\dot{\Upsilon}_i(e_{\phi_i}) \tag{37}$$

where $\chi_i = c_2\text{sign}(\dot{\mathcal{E}}_i)\left|\dot{\mathcal{E}}_i\right|^{a_2}$ and $N_i = \varrho_2\text{sign}(\dot{e}_{\phi_i})\left|\dot{e}_{\phi_i}\right|^{a_2}$.

According to (27), we have:

$$\dddot{\mathcal{E}}_i = R_i(\dddot{e}_{d_i} + \dddot{\sigma}_i) + 2\dot{R}_i(\ddot{e}_{d_i} + \ddot{\sigma}_i) + \ddot{R}_i(\dot{e}_{d_i} + \dot{\sigma}_i) \tag{38}$$

with

$$\dddot{e}_{d_i} = \dddot{M}_i - \dddot{a}_iX_i - a_i\dddot{X}_i \tag{39}$$

where $M_i = \frac{\Gamma_i - \dot{e}_{d_i}^2}{d_i}$.

Then combining with (1), (3), and (29) and (38) yields:

$$\begin{aligned}\dddot{\mathcal{E}}_i = &R_i\left[\dddot{M}_i - \dddot{a}_iX_i - a_i\dddot{X}_i - X_i\left[\frac{1}{m_i\tau_i}u_{d_i} + f_{i0} + D_i\right] + \dddot{\sigma}_i\right]\\ &+\ddot{R}_i(\dot{e}_{d_i} + \sigma_i) + 2\dot{R}_i(\ddot{e}_{d_i} + \dot{\sigma}_i).\end{aligned} \tag{40}$$

Further, the derivative of the sliding mode surface $S_{d_i}$ becomes:

$$\dot{S}_{d_i} = R_iX_i\left[-\frac{1}{m\tau_i}u_{d_i} - D_i\right] + Z_{i,1} \tag{41}$$

with

$$\begin{aligned}Z_{i,1} = &R_i\left(\dddot{M}_i - \dddot{a}_iX_i - a_i\dddot{X}_i - X_if_{i0} + \dddot{\sigma}_i\right) + \ddot{R}_i(\dot{e}_i + \sigma_i)\\ &+2\dot{R}_i(\ddot{e}_{d_i} + \dot{\sigma}_i) + \dot{\chi}_i + c_1\dot{\Upsilon}_i(\mathcal{E}_i).\end{aligned}$$

Similarly, based on (1), (9), (37), taking the derivative of the sliding mode surface $S_{\phi_i}$, we can obtain:

$$\begin{aligned}\dot{S}_{\phi_i} &= \dddot{e}_{\phi_i} + \dot{N}_i + \varrho_1\dot{\Upsilon}_i(e_{\phi_i})\\ &= \dddot{\varpi}_i - \dddot{\varphi}_i + \dot{N}_i + \varrho_1\dot{\Upsilon}_i(e_{\phi_i})\\ &= u_{\phi_i} + d_{\phi_i} - \dddot{\varphi}_i + \dot{N}_i + \varrho_1\dot{\Upsilon}_i(e_{\phi_i})\\ &= u_{\phi_i} + d_{\phi_i} + Z_{i,2}\end{aligned} \tag{42}$$

with

$$Z_{i,2} = -\dddot{\varphi}_i + \dot{N}_i + \varrho_1\dot{\Upsilon}_i(e_{\phi_i}).$$

To guarantee the convergence performance of (32) and (33), the following reaching laws are considered:

$$\begin{aligned}\dot{S}_{d_i} &= -k_{i1}\left|S_{d_i}\right|^{\rho}\text{sign}(S_{d_i}) - k_{i2}S_{d_i}\\ \dot{S}_{\phi_i} &= -k_{i3}\left|S_{\phi_i}\right|^{\rho}\text{sign}(S_{\phi_i}) - k_{i4}S_{\phi_i}\end{aligned} \tag{43}$$

where $k_{i1}$, $k_{i2}$, $k_{i3}$, $k_{i4}$ and $\rho$ are positive constants with $0 < \rho < 1$, $k_{i2} > 1$ and $k_{i4} > 1$.

As mentioned earlier, the parameters $D_{i0}$ and $d_{i\phi 0}$ are unknown constants, thus the adaptive technique is employed to estimate the boundaries of these parameters. Define the estimation errors as

$$\begin{aligned}\tilde{\eta}_i &= \eta_i - \hat{\eta}_i\\ \tilde{\omega}_i &= \omega_i - \hat{\omega}_i\end{aligned} \tag{44}$$

where $\hat{\eta}_i$ and $\hat{\omega}_i$ are the estimates of $\eta_i$ and $\omega_i$ defined below:

$$\begin{aligned}\eta_i &\geq D_{i0}\\ \omega_i &\geq d_{\phi_{i0}}.\end{aligned} \tag{45}$$

Then, based on the reaching laws (43), the finite-time sliding mode controllers are designed as:

$$\begin{aligned}u_{d_i} &= \frac{m_i\tau_i}{X_iR_i}\left(k_{i1}\left|S_{d_i}\right|^{\rho}\text{sign}(S_{d_i}) + k_{i2}S_{d_i} + R_iX_i\hat{\eta}_i + Z_{i,1}\right)\\ u_{\phi_i} &= -k_{i3}\left|S_{\phi_i}\right|^{\rho}\text{sign}(S_{\phi_i}) - k_{i4}S_{\phi_i} - Z_{i,2} - \hat{\omega}_i\end{aligned} \tag{46}$$

and the following adaptation laws:

$$\begin{aligned}\dot{\hat{\eta}}_i &= S_{d_i} R_i X_i - \sigma_{i\eta 1}\hat{\eta}_i - \sigma_{i\eta 2}\hat{\eta}_i^{\rho}\\ \dot{\hat{\omega}}_i &= S_{\phi_i} - \sigma_{i\omega 1}\hat{\omega}_i - \sigma_{i\omega 2}\hat{\omega}_i^{\rho}\end{aligned} \tag{47}$$

where $\sigma_{i\eta 1}$, $\sigma_{i\eta 2}$, $\sigma_{i\omega 1}$ and $\sigma_{i\omega 2}$ are positive parameters.

### C. Stability Analysis

*Theorem 1:* Consider the 2-D plane vehicular platoon (1) and (4) under Assumption 1. By adopting the given control schemes, including the prescribed performance control mechanism (17)–(26), the controllers (46), and the adaptation laws (47), the following objectives are achieved.

1) The closed-loop vehicular system can achieve finite-time stable within a time $T$, and the tracking errors $e_{d_i}$ and $e_{\phi_i}$, $(i \in \mathcal{V}_N)$ will converge to a neighborhood of origin in a finite time $T$.
2) The performance constraints (17) are not violated.
3) Finite-time weak string stability within a given time $\tilde{T}$ can be guaranteed.

*Proof:* The proof consists of the following three parts.

*Part 1: Boundedness of $e_{d_i}$ and $e_{\phi_i}$:* Choose the following Lyapunov function candidate:

$$V_i = \frac{1}{2}S_{d_i}^2 + \frac{1}{2}S_{\phi_i}^2 + \frac{1}{2}\tilde{\eta}_i^2 + \frac{1}{2}\tilde{\omega}_i^2. \tag{48}$$

Taking the derivative of $V_i$, combining with (41) and (42), we have:

$$\begin{aligned}\dot{V}_i =& \; S_{d_i}\dot{S}_{d_i} + S_{\phi_i}\dot{S}_{\phi_i} - \tilde{\eta}_i\dot{\hat{\eta}}_i - \tilde{\omega}_i\dot{\hat{\omega}}_i\\ =& \; S_{d_i}\left[R_i X_i\left(-\frac{1}{m_i\tau_i}u_{d_i} - D_i\right) + Z_{i,1}\right]\\ &+ S_{\phi_i}\left(u_{\phi_i} + d_{\phi_i} + Z_{i,2}\right) - \tilde{\eta}_i\dot{\hat{\eta}}_i - \tilde{\omega}_i\dot{\hat{\omega}}_i.\end{aligned} \tag{49}$$

Based on (41), one can obtain

$$S_{d_i}\dot{S}_{d_i} = S_{d_i}\left[R_i X_i\left(-\frac{1}{m_i\tau_i}u_{d_i} - D_i\right) + Z_{i,1}\right]. \tag{50}$$

Substituting (46) into (50) yields

$$\begin{aligned}S_{d_i}\dot{S}_{d_i} =& \; -k_{i1}\left|S_{d_i}\right|^{\rho} S_{d_i}\mathrm{sign}\left(S_{d_i}\right) - k_{i2}S_{d_i}^2\\ &- S_{d_i}R_i X_i\hat{\eta}_i - S_{d_i}R_i X_i D_i.\end{aligned} \tag{51}$$

Similarly, based on (42) and (46), we have

$$\begin{aligned}S_{\phi_i}\dot{S}_{\phi_i} &= S_{\phi_i}\left(u_{\phi_i} + d_{\phi_i} + Z_{i,2}\right)\\ &= -k_{i3}\left|S_{\phi_i}\right|^{\rho} S_{\phi_i}\mathrm{sign}\left(S_{\phi_i}\right) - k_{i4}S_{\phi_i}^2\\ &\quad + S_{\phi_i}d_{\phi_i} - S_{\phi_i}\hat{\omega}_i.\end{aligned} \tag{52}$$

According to (45), the following inequalities hold:

$$\begin{aligned}-S_{d_i}R_i X_i D_i &\le \left|S_{d_i}X_i\right|R_i\eta_i\\ S_{\phi_i}d_{\phi_i} &\le \left|S_{\phi_i}\right|\omega_i.\end{aligned} \tag{53}$$

Then, we have

$$\begin{aligned}S_{d_i}\dot{S}_{d_i} \le& \; -k_{i1}\left|S_{d_i}\right|^{\rho} S_{d_i}\mathrm{sign}\left(S_{d_i}\right) - k_{i2}S_{d_i}^2\\ &- S_{d_i}R_i X_i\hat{\eta}_i + \left|S_{d_i}X_i\right|R_i\eta_i\end{aligned}$$

$$\begin{aligned}S_{\phi_i}\dot{S}_{\phi_i} \le& \; -k_{i3}\left|S_{\phi_i}\right|^{\rho} S_{\phi_i}\mathrm{sign}\left(S_{\phi_i}\right) - k_{i4}S_{\phi_i}^2\\ &+ \left|S_{\phi_i}\right|\omega_i - S_{\phi_i}\hat{\omega}_i.\end{aligned} \tag{54}$$

Based on (47), we can obtain:

$$\begin{aligned}-\tilde{\eta}_i\dot{\hat{\eta}}_i =& \; -S_{d_i}R_i X_i\tilde{\eta}_i + \sigma_{i\eta 1}\hat{\eta}_i\tilde{\eta}_i + \sigma_{i\eta 2}\hat{\eta}_i^{\rho}\tilde{\eta}_i\\ -\tilde{\omega}_i\dot{\hat{\omega}}_i =& \; -S_{\phi_i}\tilde{\omega}_i + \sigma_{i\omega 1}\hat{\omega}_i\tilde{\omega}_i + \sigma_{i\omega 2}\hat{\omega}_i^{\rho}\tilde{\omega}_i.\end{aligned} \tag{55}$$

According to Lemma 4, the following inequalities hold:

$$\begin{aligned}\sigma_{i\eta 1}\hat{\eta}_i\tilde{\eta}_i &\le \frac{\sigma_{i\eta 1}}{2}\eta_i^2 - \frac{\sigma_{i\eta 1}}{2}\tilde{\eta}_i^2\\ \sigma_{i\omega 1}\hat{\omega}_i\tilde{\omega}_i &\le \frac{\sigma_{i\omega 1}}{2}\omega_i^2 - \frac{\sigma_{i\omega 1}}{2}\tilde{\omega}_i^2.\end{aligned} \tag{56}$$

Similarly, by using Lemma 3, we can obtain:

$$\begin{aligned}\sigma_{i\eta 2}\hat{\eta}_i^{\rho}\tilde{\eta}_i &\le -\frac{\sigma_{i\eta 2}}{1+\rho}\tilde{\eta}_i^{1+\rho} + \frac{2\sigma_{i\eta 2}}{1+\rho}\eta_i^{1+\rho}\\ \sigma_{i\omega 2}\hat{\omega}_i^{\rho}\tilde{\omega}_i &\le -\frac{\sigma_{i\omega 2}}{1+\rho}\tilde{\omega}_i^{1+\rho} + \frac{2\sigma_{i\omega 2}}{1+\rho}\omega_i^{1+\rho}.\end{aligned} \tag{57}$$

Substituting (51)–(57) into (49), $\dot{V}_i$ becomes:

$$\begin{aligned}\dot{V}_i \le& \; -k_{i1}\left|S_{d_i}\right|^{\rho+1} - k_{i3}\left|S_{\phi_i}\right|^{\rho+1} - k_{i2}S_{d_i}^2 - k_{i4}S_{\phi_i}^2\\ &+ \frac{\sigma_{i\eta 1}}{2}\eta_i^2 - \frac{\sigma_{i\eta 1}}{2}\tilde{\eta}_i^2 - \frac{\sigma_{i\eta 2}}{1+\rho}\tilde{\eta}_i^{1+\rho} + \frac{2\sigma_{i\eta 2}}{1+\rho}\eta_i^{1+\rho}\\ &+ \frac{\sigma_{i\omega 1}}{2}\omega_i^2 - \frac{\sigma_{i\omega 1}}{2}\tilde{\omega}_i^2 - \frac{\sigma_{i\omega 2}}{1+\rho}\tilde{\omega}_i^{1+\rho} + \frac{2\sigma_{i\omega 2}}{1+\rho}\omega_i^{1+\rho}\\ &- S_{d_i}R_i X_i\hat{\eta}_i + \left|S_{d_i}X_i\right|R_i\eta_i - S_{d_i}R_i X_i\tilde{\eta}_i\\ &+ \left|S_{\phi_i}\right|\omega_i - S_{\phi_i}\hat{\omega}_i - S_{\phi_i}\tilde{\omega}_i.\end{aligned} \tag{58}$$

Based on (44), we have

$$\begin{aligned}&- S_{d_i}R_i X_i\hat{\eta}_i + \left|S_{d_i}X_i\right|R_i\eta_i - S_{d_i}R_i X_i\tilde{\eta}_i\\ &= \left|S_{d_i}X_i\right|R_i\eta_i - S_{d_i}R_i X_i\eta_i\\ &\le 2\left|S_{d_i}X_i\right|R_i\eta_i.\end{aligned} \tag{59}$$

Using Young's inequality, we further have

$$\left|S_{d_i}X_i\right|R_i\eta_i \le \frac{1}{2}S_{d_i}^2 + \frac{1}{2}X_i^2R_i^2\eta_i^2. \tag{60}$$

Similarly, we also have

$$\begin{aligned}-S_{\phi_i}\hat{\omega}_i + \left|S_{\phi_i}\right|\omega_i - S_{\phi_i}\tilde{\omega}_i &= \left|S_{\phi_i}\right|\omega_i - S_{\phi_i}\omega_i\\ &\le S_{\phi_i}^2 + \omega_i^2.\end{aligned} \tag{61}$$

Further, one has:

$$\begin{aligned}\dot{V}_i \le& \; -2^{\frac{\rho+1}{2}}k_{i1}\left(\frac{1}{2}S_{d_i}^2\right)^{\frac{\rho+1}{2}} - 2^{\frac{\rho+1}{2}}k_{i3}\left(\frac{1}{2}S_{\phi_i}^2\right)^{\frac{\rho+1}{2}}\\ &- 2(k_{i2}-1)\left(\frac{1}{2}S_{d_i}^2\right) - 2(k_{i4}-1)\left(\frac{1}{2}S_{\phi_i}^2\right)\\ &- 2^{\frac{\rho+1}{2}}\frac{\sigma_{i\eta 2}}{1+\rho}\left(\frac{1}{2}\tilde{\eta}_i^2\right)^{\frac{\rho+1}{2}} - 2^{\frac{\rho+1}{2}}\frac{\sigma_{i\omega 2}}{1+\rho}\left(\frac{1}{2}\tilde{\omega}_i^2\right)^{\frac{\rho+1}{2}}\\ &- \sigma_{i\eta 1}\left(\frac{1}{2}\tilde{\eta}_i^2\right) - \sigma_{i\omega 1}\left(\frac{1}{2}\tilde{\omega}_i^2\right) + \left(X_i^2R_i^2 + \frac{\sigma_{i\eta 1}}{2}\right)\eta_i^2\end{aligned}$$

$$+\frac{2\sigma_{i\eta 2}}{\rho+1}\eta_i^{\rho+1}+\frac{\sigma_{i\omega 1}+2}{2}\omega_i^2+\frac{2\sigma_{i\omega 2}}{\rho+1}\omega_i^{\rho+1}. \tag{62}$$

In the light of Lemma 2, we have:

$$\begin{aligned}\dot{V}_i \leq & -\beta_i\left[\left(\frac{1}{2}S_{d_i}^2\right)^{\frac{\rho+1}{2}}+\left(\frac{1}{2}S_{\phi_i}^2\right)^{\frac{\rho+1}{2}}+\left(\frac{1}{2}\tilde{\eta}_i^2\right)^{\frac{\rho+1}{2}}\right.\\ &\left.+\left(\frac{1}{2}\tilde{\omega}_i^2\right)^{\frac{\rho+1}{2}}\right]-\lambda_i\left[\frac{1}{2}S_{d_i}^2+\frac{1}{2}S_{\phi_i}^2+\frac{1}{2}\tilde{\eta}_i^2+\frac{1}{2}\tilde{\omega}_i^2\right]\\ \leq & -\beta_i V_i^{\frac{\rho+1}{2}}-\lambda_i V_i+C_i\end{aligned} \tag{63}$$

where

$$\begin{aligned}\beta_i=&\ 2^{\frac{\rho+1}{2}}\min\left\{k_{i1},k_{i3},\frac{\sigma_{i\eta 2}}{\rho+1},\frac{\sigma_{i\omega 2}}{\rho+1}\right\}\\ \lambda_i=&\ \min\left\{2(k_{i2}-1),2(k_{i4}-1),\sigma_{i\eta 1},\sigma_{i\omega 1}\right\}\\ C_i=&\ \left(X_i^2R_i^2+\frac{\sigma_{i\eta 1}}{2}\right)\eta_i^2+\frac{2\sigma_{i\eta 2}}{\rho+1}\eta_i^{\rho+1}+\frac{\sigma_{i\omega 1}+2}{2}\omega_i^2\\ &+\frac{2\sigma_{i\omega 2}}{\rho+1}\omega_i^{\rho+1}.\end{aligned}$$

According to Lemma 1, we know that $V_i$ is PFnTS, and there must exist a constant $\kappa_i$ that satisfies $0<\kappa_i<1$, such that $S_{d_i}$, $S_{\phi_i}$, $\tilde{\eta}_i$ and $\tilde{\omega}_i$ tend to the region $\Omega_i$ in finite time $T_{i1}$, wherein $\Omega_i$ and $T_{i1}$ are as follows:

$$\begin{aligned}\left|S_{d_i}\right|,\left|S_{\phi_i}\right|,|\tilde{\eta}_i|,|\tilde{\omega}_i|\leq\Omega_i=\min\left\{\sqrt{\frac{2C_i}{(1-\kappa_i)\lambda_i}},\right.\\ \left.\sqrt{2\left(\frac{C_i}{(1-\kappa_i)\beta_i}\right)^{\frac{2}{1+\rho}}}\right\}\end{aligned} \tag{64}$$

and

$$\begin{aligned}T_{i1}\leq\max\left\{\frac{2}{\kappa_i\lambda_i(1-\rho)}\ln\frac{\kappa_i\lambda_i V_i^{\frac{1-\rho}{2}}(0)+\beta_i}{\beta_i},\right.\\ \left.\frac{2}{\lambda_i(1-\rho)}\ln\frac{\lambda_i V_i^{\frac{1-\rho}{2}}(0)+\kappa_i\beta_i}{\kappa_i\beta_i}\right\}.\end{aligned} \tag{65}$$

Therefore, for the platoon systems, all signals $S_{d_i}$, $S_{\phi_i}$, $\tilde{\eta}_i$ and $\tilde{\omega}_i$ are bounded in finite-time.

According to (64), by choosing the appropriate design parameters, it is guaranteed that $S_{d_i}$ and $S_{\phi_i}$ converges to a smaller domain near zero when $t\geq T_{i1}$, that is $S_{d_i}\approx 0$, $S_{\phi_i}\approx 0$. Then, sliding mode surfaces (32) and (33) become:

$$\ddot{\mathcal{E}}_i(t)+c_2\text{sign}(\dot{\mathcal{E}}_i)\left|\dot{\mathcal{E}}_i\right|^{a_2}+c_1\Upsilon_i(\mathcal{E}_i)=0 \tag{66}$$

$$\ddot{e}_{\phi_i}+\varrho_2\text{sign}(\dot{e}_{\phi_i})\left|\dot{e}_{\phi_i}\right|^{a_2}+\varrho_1\Upsilon_i(e_{\phi_i})=0. \tag{67}$$

And then, on the basis of (34), we will discuss the convergence of $\mathcal{E}_i$ and $e_{\phi_i}$ from the following two cases. Here, the analysis for $e_{\phi_i}$ is the same as for $\mathcal{E}_i$, thus only the convergence of $\mathcal{E}_i$ is analyzed for save space.

*Case 1:* When $\left|\mathcal{E}_i\right|\geq\iota_i$, (66) becomes:

$$\ddot{\mathcal{E}}_i(t)+c_2\text{sign}(\dot{\mathcal{E}}_i)\left|\dot{\mathcal{E}}_i\right|^{a_2}+c_1\text{sig}^{a_1}(\mathcal{E}_i)=0 \tag{68}$$

Based on [39], it is obvious that, by configuring the parameters $c_1$, $c_2$, $a_1$, $a_2$ that satisfy the conditions as given in (34) and (35), $\mathcal{E}_i(t)$ and $e_{\phi_i}$can converge to zero along the sliding mode surfaces $S_{d_i}=0$ and $S_{\phi_i}=0$ in finite-time $T_{d_i2}$ and $T_{\phi_i2}$, respectively. Therefore, we have: $T_{i2}=\max\{T_{d_i2},T_{\phi_i2}\}$.

*Case 2:* When $\left|\mathcal{E}_i\right|<\iota_i$, rewrite (66) as:

$$\ddot{\mathcal{E}}_i(t)+c_2\text{sign}(\dot{\mathcal{E}}_i)\left|\dot{\mathcal{E}}_i\right|^{a_2}+c_1\left(\alpha_1\mathcal{E}_i+\alpha_2\mathcal{E}_i^2\text{sign}(\mathcal{E}_i)\right)=0 \tag{69}$$

As analyzed in [21], if parameters $\alpha_1$ and $\alpha_2$ are chosen as (34), $\dot{\mathcal{E}}_i=-c_1(\alpha_1\mathcal{E}_i+\alpha_2\mathcal{E}_i^2\text{sign}(\mathcal{E}_i))$ has a faster convergence rate than $\dot{\mathcal{E}}_i=-c_1|\mathcal{E}_i|^{a_1}\text{sign}(\mathcal{E}_i)$. Thus, a shorter convergence time can be obtained.

Given the above analysis, the errors $\mathcal{E}_i$ and $e_{\phi_i}$ are finite time stable, that is $\mathcal{E}_i$ and $e_{\phi_i}$ converge to a small region near origin in finite time $T_i\leq T_{i1}+T_{i2}$.

Since $\mathcal{E}_i$ and $e_{d_i}$ are equivalent, thus the finite-time convergence of $e_{d_i}$ is also realized within the time $T_i$.

*Part 2: Reachability of prescribed performance (17):* From equation (25), it can be deduced that:

$$e^{\mathcal{E}_i}=\begin{cases}\frac{e_{d_i}(t)-\overline{B}_i(t)}{\overline{A}_i(t)-e_{d_i}(t)}, & e_{d_i}(0)\geq 0\\ \frac{e_{d_i}(t)-\underline{A}_i(t)}{\underline{B}_i(t)-e_{d_i}(t)}, & e_{d_i}(0)<0\end{cases} \tag{70}$$

Further, we can obtain:

$$\frac{e^{\varepsilon_i}}{1+e^{\varepsilon_i}}=\begin{cases}\frac{e_{d_i}(t)-\overline{B}_i(t)}{\overline{A}_i(t)-\overline{B}_i(t}, & e_{d_i}(0)\geq 0\\ \frac{e_{d_i}(t)-\underline{A}_i(t)}{\underline{B}_i(t)-\underline{A}_i(t)}, & e_{d_i}(0)<0\end{cases} \tag{71}$$

Definite $\overline{\mathcal{E}}_i$ as the upper bound of $\mathcal{E}_i$, the following inequalities holds:

$$0<\frac{e^{-\bar{\mathcal{E}}_i}}{1+e^{-\bar{\mathcal{E}}_i}}<\frac{e_i^{\mathcal{E}}}{1+e_i^{\mathcal{E}}}<\frac{e^{\bar{\mathcal{E}}_i}}{1+e^{\bar{\mathcal{E}}_i}}<1$$

Then

$$\begin{cases}0<\frac{e_{d_i}(t)-\overline{B}_i(t)}{\overline{A}_i(t)-\overline{B}_i(t)}<1, & e_{d_i}(0)\geq 0\\ 0<\frac{e_{d_i}(t)-\underline{A}_i(t)}{\underline{B}_i(t)-\underline{A}_i(t)}<1, & e_{d_i}(0)<0\end{cases} \tag{72}$$

After calculation we can get:

$$\begin{cases}\overline{A}_i(t)<e_{d_i}(t)<\overline{B}_i(t), & e_{d_i}(0)\geq 0\\ \underline{B}_i(t)<e_{d_i}(t)<\underline{A}_i(t), & e_{d_i}(0)<0\end{cases} \tag{73}$$

Therefore, when stability of $\mathcal{E}_i$ is achieved, the predefined tracking performance (17) can be guaranteed.

*Part 3: Weak string stability:* Based on (17)–(21), the tracking error $e_{d_i}$ converges to the predefined region $(-\epsilon_i,\epsilon_i)$ when $t\geq\tilde{T}_i$, that is $|e_{d_i}(t)|<\epsilon_i$ for $\forall t\geq\tilde{T}_i$. Based on Definition 1, we can obtain that the vehicular platoon system is finite-time weak string stability.

The whole proof of Theorem 1 is accomplished by the above three parts. ■

## IV. Simulation Studies

To demonstrate the effectiveness of the developed scheme, numerical simulations are carried out for a vehicular platoon system with four following vehicles and one leader. In the simulation, the parameters of vehicle $i$ are set as follows: $m_i = 1605\,\text{kg}$, $\tau_i = 0.2$, $A_i = 2.2\,\text{m}^2$, $\rho_{ai4} = 0.2$, $C_{ai} = 0.35$, $g = 9.8\,\text{m/s}^2$, $\delta_i = 0$, $b_i = 0.02$, $d_i(t) = 0.1\tanh(t)$, $\Delta f_i(x_i, y_i, v_i, a_i) = 0.5 f_{i0}(x_i, y_i, v_i, a_i)$. The platoon parameters are chosen as: $d_i^* = 15\,\text{m}$, $d_{i\min} = 9\,\text{m}$ and $d_{i\max} = 23\,\text{m}$. The leader drives by the following acceleration:

$$a_0(t) = \begin{cases} 0.4\text{t m/s}^2, & 0\text{s} \le \text{t} < 5\text{s} \\ 2\ \text{m/s}^2, & 5\text{s} \le \text{t} < 9\text{s} \\ -0.4t + 6\ \text{m/s}^2, & 9\text{s} \le \text{t} < 12\text{s} \\ 0\ \text{m/s}^2, & t \ge 12\text{s} \end{cases} \tag{74}$$

### A. Simulation Results of the Proposed Control Scheme

Based on the platoon parameters, the FnTPFs are constructed as:

$$\overline{A}_i(t) = \begin{cases} (8-0.2)\dfrac{1-\frac{t}{25}}{\ln\left(e+\frac{25t}{25-t}\right)} + 0.2, & 0 \le t \le 25 \\ 0.2, & t > 25 \end{cases} \tag{75}$$

$$\underline{A}_i(t) = \begin{cases} (-6+0.2)\dfrac{1-\frac{t}{25}}{\ln\left(e+\frac{25t}{25-t}\right)} - 0.2, & 0 \le t \le 25 \\ -0.2, & t > 25 \end{cases} \tag{76}$$

$$\overline{B}_i(t) = \begin{cases} (e_{d_i}(0) - 0.1 + 0.2)\,\frac{25-t}{25}\exp\left(\frac{-t}{25-t}\right) - 0.2, & 0 \le t \le 25 \\ -0.2, & t > 25 \end{cases} \tag{77}$$

$$\underline{B}_i(t) = \begin{cases} (e_{d_i}(0) + 0.1 - 0.2)\,\frac{25-t}{25}\exp\left(\frac{-t}{25-t}\right) + 0.2, & 0 \le t \le 25 \\ 0.2, & t > 25 \end{cases} \tag{78}$$

In this subsection, the following two real scenarios, i.e., multilane vehicle merging (as shown in Fig. 2) and vehicular platoon lane change (as shown in Fig. 3), are considered.

*Multilane Vehicle Merging:* In this case, the initial states of each vehicle and the control parameters are given in Tables II and III, respectively.

Simulation results of the proposed control scheme in Theorem 1 are shown in Fig. 4. Fig. 4(a) and (b) show the position and heading of each vehicle, respectively, and it is obvious that the platoon can be achieved in finite time, and no collisions occurs between adjacent vehicles. The velocity $v_i$ and angle velocity $\omega_i$ are given in Fig. 4(c) and (d), which illustrates that following vehicles eventually track these two states of the leader with bounded error. Fig. 4(e) and (f) shows that $S_{\phi_i}$ and $S_{d_i}$ converges to the neighborhood of the origin in finite time. From Fig. 4(h), The tracking error is always within the specified area and has a small overshoot, the performance function transforms the convergence region according to the initial value of the tracking error, so that the error converges quickly and smoothly to the predetermined region within a predefined time. The tracking errors converge to a region near zero in finite time ($t \le 25$), and satisfies $|e_{d_i}(t)| < \epsilon_i$, which means individual vehicle stability and string stability are obtained.

TABLE II
The Initial Conditions of Each Vehicle

| $i$ | 0 | 1 | 2 | 3 | 4 |
|---|---|---|---|---|---|
| $x_i(m)$ | 100 | 86 | 72 | 58 | 44 |
| $y_i(m)$ | 30 | 28 | 32 | 29 | 32.5 |
| $v_i(m/s)$ | 0 | 0.5 | 0.5 | 0.5 | 0.5 |
| $a_i(m/s^2)$ | 0 | 0 | 0 | 0 | 0 |
| $\phi_i(rad)$ | 0 | 0 | 0 | 0 | 0 |
| $\omega_i(rad/s)$ | 0 | 0 | 0 | 0 | 0 |
| $\varpi_i(rad/s^2)$ | 0 | 0 | 0 | 0 | 0 |

TABLE III
Control Parameters for Followers

| Parameter Name | Simulation Values |
|---|---|
| $k_{i1}, i = 1,2,3,4$ | $k_{11} = 45$, $k_{21} = 40$, $k_{31} = 45$, $k_{41} = 40$ |
| $k_{i2}, i = 1,2,3,4$ | $k_{12} = 30$, $k_{22} = 30$, $k_{32} = 30$, $k_{42} = 25$ |
| $k_{i3}, i = 1,2,3,4$ | $k_{13} = 4$, $k_{23} = 4$, $k_{33} = 4$, $k_{43} = 4$ |
| $k_{i4}, i = 1,2,3,4$ | $k_{14} = 2$, $k_{24} = 2$, $k_{34} = 2$, $k_{44} = 2$ |
| $\iota_i, i = 1,2,3,4$ | $\iota_1 = 0.05$, $\iota_2 = 0.05$, $\iota_3 = 0.05$, $\iota_4 = 0.05$ |
| $\varsigma_i, i = 1,2,3,4$ | $\varsigma_1 = 0.05$, $\varsigma_2 = 0.05$, $\varsigma_3 = 0.05$, $\varsigma_4 = 0.05$ |
| $\rho$, $a$, $c_1$, $c_2$ | $\rho = 0.6$, $a = 0.85$, $c_1 = 10$, $c_2 = 7$ |
| $\varrho_1$, $\varrho_2$, $\sigma_{i\eta 1}$, $\sigma_{i\eta 2}$ | $\varrho_1 = 10$, $\varrho_2 = 7$, $\sigma_{i\eta 1} = 0.7$, $\sigma_{i\eta 2} = 0.01$ |
| $\sigma_{i\omega 1}$, $\sigma_{i\omega 2}$ | $\sigma_{i\omega 1} = 0.7$, $\sigma_{i\omega 2} = 0.01$ |

The whole multilane vehicle merging process is given in Fig. 5. It is observed that under the proposed control strategy, the following vehicles all reach the second lane where the leader is located within 5s, and eventually forming a platoon within 15 s, completing the multilane vehicle merging task.

*Vehicular Platoon Lane Change:* To show the lane change process, the heading angle of the leader vehicle is adopted as follows:

$$\phi_0(t) = \begin{cases} 0.00167t, & 18\text{s} \le \text{t} < 22\text{s} \\ -0.00052t, & 50\text{s} \le \text{t} < 55\text{s} \\ 0, & \text{otherwise} \end{cases} \tag{79}$$

and the initial conditions of each vehicle are given in Table IV.

Fig. 6 shows the 2-D plane trajectory of platoon lane changing maneuver. It is observed that under the control scheme proposed in this paper, the lane change task can also be realized.

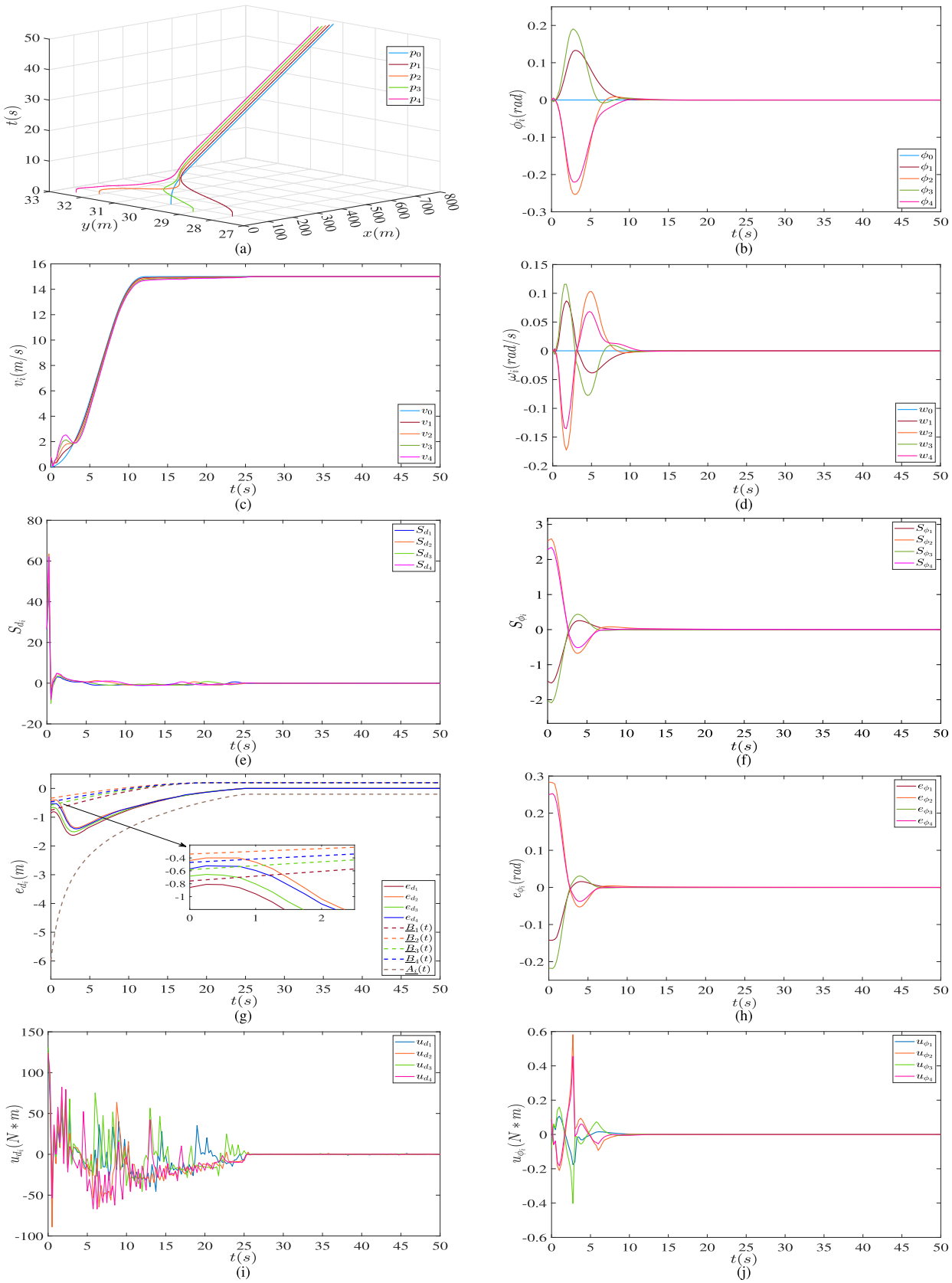


Fig. 4. Simulation results of Theorem 1 with the acceleration (74). (a) Position $p_i(t)$. (b) Heading angle $\phi_i(t)$. (c) Velocity $v_i(t)$. (d) Angular velocity $\omega_i(t)$. (e) Sliding mode surface $S_{d_i}(t)$. (f) Sliding mode surface $S_{\phi_i}(t)$. (g) Disturbance tracking error $e_{d_i}(t)$. (h) Angular tracking error $e_{\phi_i}(t)$. (i) Distance control input $u_{d_i}(t)$. (j) Angular control input $u_{\phi_i}(t)$.

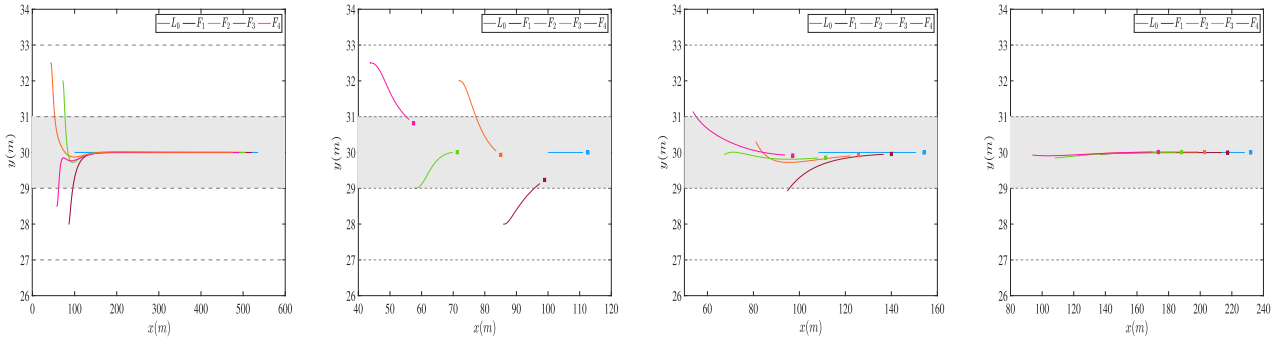


Fig. 5. Simulation results of the multilane vehicle merging. (a) time 0–35 s (b) time 0–5 s. (c) time 5–10 s. (d) time 10–15 s.

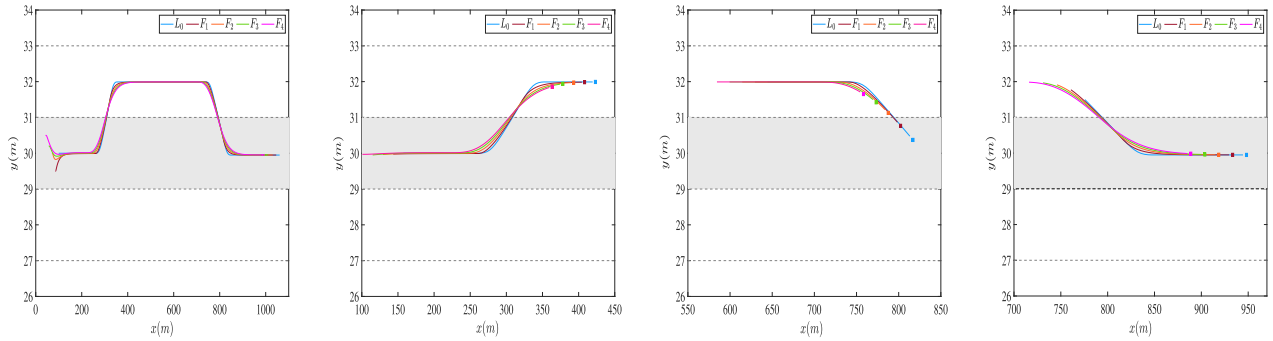


Fig. 6. Simulation results of the vehicular platoon lane changing. (a) time 0–70 s. (b) time 10–27 s. (c) time 42–54 s. (d) time 53–63 s.

TABLE IV
THE INITIAL CONDITIONS OF EACH VEHICLE

| $i$ | 0 | 1 | 2 | 3 | 4 |
|---|---|---|---|---|---|
| $x_i(m)$ | 100 | 86 | 72 | 58 | 44 |
| $y_i(m)$ | 30 | 29.5 | 30 | 30.2 | 30.5 |
| $v_i(m/s)$ | 0 | 1.5 | 1.5 | 1.5 | 1.5 |
| $a_i(m/s^2)$ | 0 | 0 | 0 | 0 | 0 |
| $\phi_i(rad)$ | 0 | 0 | 0 | 0 | 0 |
| $\omega_i(rad/s)$ | 0 | 0 | 0 | 0 | 0 |
| $\varpi_i(rad/s^2)$ | 0 | 0 | 0 | 0 | 0 |

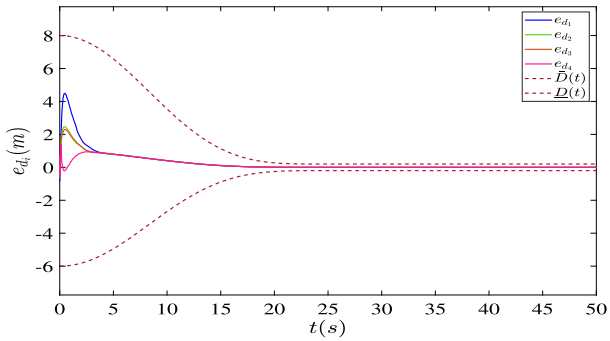


Fig. 7. The result of comparison.

### B. Simulation Comparisons

To demonstrate the superiority of the proposed algorithm, a comparison is made with the PPC method in [28]. Here, the FnTPFs adopted in [28] is given as follows:

$$\overline{D}(t) = \begin{cases} 7.8\sin^4\left(\frac{\pi}{40}(25-t)\right) + 0.2, & 0 \le t \le 25 \\ 0.2, & t > 25 \end{cases} \tag{80}$$

$$\underline{D}(t) = \begin{cases} 5.8\sin^4\left(\frac{\pi}{40}(25-t)\right) + 0.2, & 0 \le t \le 25 \\ 0.2, & t > 25 \end{cases} \tag{81}$$

Simulation result is shown in Fig. 7. By comparing Figs. 4(g), Fig. 7 and Table V, it can be found that the FnTPPC method proposed in this paper has a smaller overshoot.

TABLE V
OVERSHOOT OF TRACKING ERROR BETWEEN VEHICLES

| Overshoot | [28] | This paper |
|---|---|---|
| $\lvert e_{d_1}(m)\rvert$ | 4.633 | 1.628 |
| $\lvert e_{d_2}(m)\rvert$ | 2.653 | 1.368 |
| $\lvert e_{d_3}(m)\rvert$ | 2.278 | 1.509 |
| $\lvert e_{d_4}(m)\rvert$ | 1.44 | 1.406 |

## V. CONCLUSION

This paper has developed a new adaptive finite time prescribed performance tracking control algorithm for 2-D plane vehicular platoon. Two pairs finite-time performance functions (FnTPFs)

are designed to guarantee the spacing tracking error converges to the prescribed region in a predetermined time with small overshoot. Then, an adaptive finite-time third-order sliding mode control scheme is proposed, which is capable of compelling all signals of the system approach to a small region neighborhood zero in finite time, while ensuring both collision avoidance and connectivity maintenance all be guaranteed. In addition, under the proposed control scheme, the weak string stability of the platoon also be guaranteed.

Noteworthy, the constraint that the convergence time depends on the initial condition of the system still exists in the proposed finite-time control scheme, we will focus on fixed-time/prescribed-time 2-D platoon control in the future. Besides, the convergence domain of the prescribed performance function adopted in this paper also relies on the initial states, eliminating this constraint is also worth exploring.

## REFERENCES


[1] S. Chu and A. Majumdar, "Opportunities and challenges for a sustainable energy future," *Nature*, vol. 488, no. 7411, pp. 294–303, Aug. 2012.

[2] J. Rios-Torres and A. A. Malikopoulos, "A survey on the coordination of connected and automated vehicles at intersections and merging at highway on-ramps," *IEEE Trans. Intell. Transp. Syst.*, vol. 18, no. 5, pp. 1066–1077, May 2017.

[3] Y. Zhao, D. Gong, S. Wen, L. Ding, and G. Guo, "A privacy-preserving-based distributed collaborative scheme for connected autonomous vehicles at multi-lane signal-free intersections," *IEEE Trans. Intell. Transp. Syst.*, vol. 25, no. 7, pp. 6824–6835, Jul. 2024.

[4] Y. Zhao, Z. Liu, and W. S. Wong, "Resilient platoon control of vehicular cyber physical systems under DoS attacks and multiple disturbances," *IEEE Trans. Intell. Transp. Syst.*, vol. 23, no. 8, pp. 10945–10956, Aug. 2022.

[5] A. Rasouli and J. K. Tsotsos, "Autonomous vehicles that interact with pedestrians: A survey of theory and practice," *IEEE Trans. Intell. Transp. Syst.*, vol. 21, no. 3, pp. 900–918, Mar. 2020.

[6] J. Zhan, Z. Ma, and L. Zhang, "Data-driven modeling and distributed predictive control of mixed vehicle platoons," *IEEE Trans. Intell. Veh.*, vol. 8, no. 1, pp. 572–582, Jan. 2023.

[7] A. Alam, B. Besselink, V. Turri, J. Mårtensson, and K. H. Johansson, "Heavy-duty vehicle platooning for sustainable freight transportation: A cooperative method to enhance safety and efficiency," *IEEE Control Syst. Mag.*, vol. 35, no. 6, pp. 34–56, Dec. 2015.

[8] Y. Zheng, S. E. Li, J. Wang, D. Cao, and K. Li, "Direct adaptive longitudinal control of vehicle platoons," *IEEE Trans. Veh. Technol.*, vol. 50, no. 1, pp. 150–161, Jan. 2001.

[9] J. Chen, H. Liang, J. Li, and Z. Lv, "Stability and scalability of homogeneous vehicular platoon: Study on the influence of information flow topologies," *IEEE Trans. Intell. Transp. Syst.*, vol. 17, no. 1, pp. 14–26, Jan. 2016.

[10] L. Xiao and F. Gao, "Effect of information delay on string stability of platoon of automated vehicles under typical information frameworks," *J. Central South Univ. Technol.*, vol. 17, no. 6, pp. 1271–1278, Dec. 2010.

[11] G. Rödönyi, "An adaptive spacing policy guaranteeing string stability in multi-brand ad hoc platoons," *IEEE Trans. Intell. Transp. Syst.*, vol. 19, no. 6, pp. 1902–1912, Jun. 2018.

[12] Z. Yang, J. Huang, D. Yang, and Z. Zhong, "Collision-free ecological cooperative robust control for uncertain vehicular platoons with communication delay," *IEEE Trans. Veh. Technol.*, vol. 70, no. 3, pp. 2153–2166, Mar. 2021.

[13] Y. Li, Y. Zhao, and S. Tong, "Adaptive fuzzy control for heterogeneous vehicular platoon systems with collision avoidance and connectivity preservation," *IEEE Trans. Fuzzy Syst.*, vol. 31, no. 11, pp. 3934–3943, Nov. 2023.

[14] K. P. Tee, S. S. Ge, and E. H. Tay, "Barrier Lyapunov functions for the control of output-constrained nonlinear systems," *Automatica*, vol. 45, no. 4, pp. 918–927, Apr. 2009.

[15] X. Yuan, B. Chen, and C. Lin, "Fuzzy adaptive output-feedback tracking control for nonlinear strict-feedback systems in prescribed finite time," *J. Franklin Inst.*, vol. 358, no. 15, pp. 7309–7332, Oct. 2021.

[16] C. P. Bechlioulis and G. A. Rovithakis, "Prescribed performance adaptive control for multi-input multi-output affine in the control nonlinear systems," *IEEE Trans. Autom. Control*, vol. 55, no. 5, pp. 1220–1226, May 2010.

[17] G. Guo and D. Li, "Adaptive sliding mode control of vehicular platoons with prescribed tracking performance," *IEEE Trans. Veh. Technol.*, vol. 68, no. 8, pp. 7511–7520, Aug. 2019.

[18] D. Li and G. Guo, "Prescribed performance concurrent control of connected vehicles with nonlinear third-order dynamics," *IEEE Trans. Veh. Technol.*, vol. 69, no. 12, pp. 14793–14802, Dec. 2020.

[19] J. Wang, X. Luo, W. Wong, and X. Guan, "Specified-time vehicular platoon control with flexible safe distance constraint," *IEEE Trans. Veh. Technol.*, vol. 68, no. 11, pp. 10489–10503, Nov. 2019.

[20] Z. Gao, Y. Zhang, and G. Guo, "Finite-time fault-tolerant prescribed performance control of connected vehicles with actuator saturation," *IEEE Trans. Veh. Technol.*, vol. 72, no. 2, pp. 1438–1448, Feb. 2023.

[21] Z. Sun, Z. Gao, G. Guo, and S. Wen, "Finite-time control of vehicular platoons with global prescribed performance and actuator nonlinearities," *IEEE Trans. Intell. Veh.*, vol. 9, no. 1, pp. 1768–1779, Jan. 2024.

[22] Z. Gao, Y. Zhang, and G. Guo, "Fixed-time prescribed performance adaptive fixed-time sliding mode control for vehicular platoons with actuator saturation," *IEEE Trans. Intell. Transp. Syst.*, vol. 23, no. 12, pp. 24176–24189, Dec. 2022.

[23] G. Cui, W. Yang, J. Yu, Z. Li, and C. Tao, "Fixed-time prescribed performance adaptive trajectory tracking control for a QUAV," *IEEE Trans. Circuits Syst. II, Exp. Briefs*, vol. 69, no. 2, pp. 494–498, Feb. 2022.

[24] Y. Li, K. Li, T. Zheng, X. Hu, H. Feng, and Y. Li, "Evaluating the performance of vehicular platoon control under different network topologies of initial states," *Phys. A., Statist. Mech. Appl.*, vol. 450, pp. 359–368, May 2016.

[25] S. L. Dai, S. He, X. Chen, and X. Jin, "Adaptive leader–follower formation control of nonholonomic mobile robots with prescribed transient and steady-state performance," *IEEE Trans. Ind. Informat.*, vol. 16, no. 6, pp. 3662–3671, Jun. 2020.

[26] D. Wang, M. Fu, S. S. Ge, and D. Li, "Velocity free platoon formationcontrol for unmanned surface vehicles with output constraints and modeluncertainties," *Appl. Sci.*, vol. 10, no. 3, 2020, Art. no. 1118.

[27] W. Xu, X. Guo, J. Wang, W. Che, and Z. Wu, "Nonlinear disturbance observer-based fault-tolerant sliding-mode control for 2-D plane vehicular platoon with UTVFD and ANAS," *IEEE Trans. Cybern.*, vol. 54, no. 4, pp. 2050–2061, Apr. 2024.

[28] L. Zhang, W. Che, S. Xu, and C. Deng, "Prescribed performance tracking control for 2-D plane vehicle platoons with actuator faults and saturations," *IEEE Trans. Veh. Technol.*, vol. 72, no. 11, pp. 14040–14050, Nov. 2023.

[29] Z. Gao, Z. Sun, and G. Guo, "Automatic adjustable fixed-time prescribed performance control of heterogeneous vehicular platoons with actuator saturation," *IEEE Trans. Intell. Transp. Syst.*, vol. 25, no. 9, pp. 12736–12748, Sep. 2024.

[30] Z. Gao, Z. Sun, and G. Guo, "Adaptive predefined-time tracking control for vehicular platoons with finite-time global prescribed performance independent of initial conditions," *IEEE Trans. Veh. Technol.*, early access, Jul. 03, 2024, doi: 10.1109/TVT. 2024.3420906.

[31] J. Wang, W. Wong, X. Luo, X. Li, and X. Guan, "Connectivity maintained and specified-time vehicle platoon control systems with disturbance observer," *Int. J. Robust Nonlinear Control*, vol. 31, no. 16, pp. 7844–7861, Aug. 2021.

[32] F. Gao, X. Hu, S. E. Li, K. Li, and Q. Sun, "Distributed adaptive sliding mode control of vehicular platoon with uncertain interaction topology," *IEEE Trans. Ind. Electron.*, vol. 65, no. 8, pp. 6352–6361, Aug. 2018.

[33] G. Guo, P. Li, and L. Hao, "Adaptive fault-tolerant control of platoons with guaranteed traffic flow stability," *IEEE Trans. Veh. Technol.*, vol. 69, no. 7, pp. 6916–6927, Jul. 2020.

[34] X. Guo, W. Xu, J. Wang, J. H. Park, and H. Yan, "BLF-based neuroadaptive fault-tolerant control for nonlinear vehicular platoon with time-varying fault directions and distance restrictions," *IEEE Trans. Intell. Transp. Syst.*, vol. 23, no. 8, pp. 12388–12398, Aug. 2022.

[35] Y. Wang, C. Liu, and L. Shan, "Fixed-time integral terminal sliding mode control for vehicle platoon with prescribed performance," *Int J. Control Autom. Syst*, vol. 22, no. 1, pp. 27–35, Jan. 2024.
[36] V. K. Tripathi, A. K. Kamath, L. Behera, N. K. Verma, and S. Nahavandi, "An adaptive fast terminal sliding-mode controller with power rate proportional reaching law for quadrotor position and altitude tracking," *IEEE Trans. Syst., Man, Cybern., Syst.*, vol. 52, no. 6, pp. 3612–3625, Jun. 2022.
[37] J. Yu, P. Shi, and L. Zhao, "Finite-time command filtered backstepping control for a class of nonlinear systems," *Automatica*, vol. 92, pp. 173–180, Jun. 2018.
[38] X. Guo, W. Xu, J. Wang, and J. H. Park, "Distributed neuroadaptive fault-tolerant sliding-mode control for 2-D plane vehicular platoon systems with spacing constraints and unknown direction faults," *Automatica*, vol. 129, Jul. 2021, Art. no. 109675.
[39] Y. Feng, F. Han, and X. Yu, "Chattering free full-order sliding-mode control," *Automatica*, vol. 50, no. 4, pp. 1310–1314, Apr. 2014.

**Zhenyu Gao** received the Ph.D degree from Dalian Maritime University, Dalian, China, in 2019. He is currently an Associate Professor with the School of Control Engineering, Northeastern University at Qinhuangdao, Qinhuangdao, China. His research interests include cooperative control of autonomous vehicles, and intelligent transportation systems.

**Zhongyang Wei** received the B.S. degree from the Shandong University of Science and Technology, Qingdao, China, in 2023. He is currently working toward the M.S. degree with the School of Control Engineering, Northeastern University at Qinhuangdao, Qinhuangdao, China. His research interests include vehicular platoon control, and intelligent transportation systems.

**Wei Liu** received the B.S. degree from Dalian Polytechnic University, Dalian, China, in 2022. He is currently working toward the M.S. degree with the School of Control Engineering, Northeastern University at Qinhuangdao, Qinhuangdao, China. His research interests include vehicular platoon control, and intelligent transportation systems.

**Ge Guo** (Senior Member, IEEE) received the B.S. and Ph.D. degrees from Northeastern University, Shenyang, China, in 1994 and 1998, respectively. He is currently a Professor with Northeastern University. He has authored or coauthored more than 130 international journal articles in his research interests which include intelligent transportation systems, cyber-physical systems, and connected automated vehicles. He was recipient of the First Prize of the Chinese Association of Automation Young Scientist Award and Hebei Province Natural Sciences Award and was also an Honoree of the Ministry of Education New Century Excellent Talents in 2004 and Nominee for Gansu Top Ten Excellent Youths. He is an Associate Editor for IEEE TRANSACTIONS ON INTELLIGENT TRANSPORTATION SYSTEMS, IEEE TRANSACTIONS ON VEHICULAR TECHNOLOGY, IEEE TRANSACTIONS ON INTELLIGENT VEHICLES, *Information Sciences*, *IEEE Intelligent Transportation Systems Magazine*, *ACTA Automatica Sinica*.